Proximal Tubules Have the Capacity to Regulate Uptake of Albumin

Mark C. Wagner,* Silvia B. Campos-Bilderback,* Mahboob Chowdhury,[†] Brittany Flores,*
Xianyin Lai,[‡] Jered Myslinski,* Sweekar Pandit,* Ruben M. Sandoval,* Sarah E. Wean,*
Yuan Wei,[§] Lisa M. Satlin,[§] Roger C. Wiggins,[†] Frank A. Witzmann,[‖] and
Bruce A. Molitoris*[‖]

*Indiana University School of Medicine, The Roudebush Veterans Affair Medical Center, Indiana Center for Biological
Microscopy, Indianapolis, Indiana; [§]Department of Pediatrics, The Icahn School of Medicine at Mount Sinai, New York;
[†]Department of Internal Medicine, University of Michigan, Ann Arbor, Michigan; [‡]Department of Biochemistry and
Molecular Biology, Indiana University School of Medicine, Indianapolis, Indiana; and [‖]Department of Cellular and
Integrative Physiology, Indiana University School of Medicine, Indianapolis, Indiana

ABSTRACT

Evidence from multiple studies supports the concept that both glomerular filtration and proximal tubule (PT) reclamation affect urinary albumin excretion rate. To better understand these roles of glomerular filtration and PT uptake, we investigated these processes in two distinct animal models. In a rat model of acute exogenous albumin overload, we quantified glomerular sieving coefficients (GSC) and PT uptake of Texas Red-labeled rat serum albumin using two-photon intravital microscopy. No change in GSC was observed, but a significant decrease in PT albumin uptake was quantified. In a second model, loss of endogenous albumin was induced in rats by podocyte-specific transgenic expression of diphtheria toxin receptor. In these albumin-deficient rats, exposure to diphtheria toxin induced an increase in albumin GSC and albumin filtration, resulting in increased exposure of the PTs to endogenous albumin. In this case, PT albumin reabsorption was markedly increased. Analysis of known albumin receptors and assessment of cortical protein expression in the albumin overload model, conducted to identify potential proteins and pathways affected by acute protein overload, revealed changes in the expression levels of calreticulin, disabled homolog 2, NRF2, angiopoietin-2, and proteins involved in ATP synthesis. Taken together, these results suggest that a regulated PT cell albumin uptake system can respond rapidly to different physiologic conditions to minimize alterations in serum albumin level.

While the clinical relevance of proteinuria, and especially albuminuria, has been well documented, the quantitative and mechanistic significance of different components to albumin excretion remains an area of considerable excitement and debate.[1] Recent data from several laboratories utilizing different approaches have delineated a role of proximal tubules (PTs) in regulation of albumin reabsorption and reclamation.[2] Furthermore, albumin transcytosis has been visualized in PT cells[3] and FcRn has been shown to mediate the transcytosis of albumin across PTCs,[4] as it is known to do for many other cell types.[2] Therefore, the present studies were conducted to begin differentiating and quantifying glomerular and PT contributions to albuminuria under physiologic and disease conditions. This understanding is important because before appropriate therapies can be developed to modulate albuminuria, the structural, functional and mechanistic characterization need to be better understood and interrelated.

PTs regulate glomerular filtrate uptake, sorting, degradation, transcytosis, and secretion, thus serving as a key contributor in determining urine composition. Further, PT cells have extremely active endocytosis mechanisms and are thus responsible for retrieving most filtered proteins under normal conditions.[5] Given the recent data supporting increased filtration of proteins (*i.e.*, albumin), understanding their endocytic mechanisms becomes even more important.[2] A clear role of megalin/cubilin in receptor-mediated clathrin-dependent endocytosis function exists and in addition there is an active non-selective fluid-phase endocytosis pathway.[6] However, the only known transcytosis receptor for albumin is FcRn.[7] While many questions remain concerning these processes it is clear that multiple diseases result from protein trafficking defects in PT.[2,8] Therefore, to begin addressing how the PTs handle filtered proteins two different rat models of proteinuria have been investigated.

First, the acute albumin overload model, which has been used for over 20 years and induces a significant rapid and reversible increase in albuminuria, was evaluated.[9,10] The second model was a transgenic rat line that specifically expresses the diphtheria toxin (DT) receptor in podocytes under the control of the podocyte-specific podocin promoter. Under physiologic conditions urinary albumin was unaltered, but the presence of DT results in selective podocyte injury/death resulting in increased albumin leak across the glomerular filtration barrier.[11]

An implicit assumption has always been that in both models albuminuria results from enhanced passage of albumin across the glomerular filtration barrier. However, recent data from multiple laboratories supports a role for both the glomerulus and PT cell in determining the level of albuminuria in disease processes.[2] Previously it had not been possible to evaluate the role of the PTC in these models. However, intravital two-photon microscopy of the kidney now permits a direct evaluation of changes occurring in glomerular filtration and PTC uptake of fluorescent molecules simultaneously in the same nephron.[12,13] An increase in the glomerular sieving coefficient (GSC) would be consistent with a glomerular effect while changes in the level of PTC uptake would support a role for the PTC in albuminuria. The ability to simultaneously monitor both mechanisms is essential for understanding the mechanism of albuminuria.

RESULTS

Albuminuria in the MWF Rats Following Albumin Overload

Initial studies were undertaken to characterize the albumin overload model in the female Munich Wistar Fromter (MWF) rats. Their superficial glomeruli have allowed our laboratory, and others, to directly observe and quantify glomerular and tubular events using intravital two-photon microscopy.[12,14] Figure 1A shows a rapid increase in plasma albumin and then recovery to baseline serum levels on days 3 and 4, as previously published,[9] when imaging was undertaken. Figure 1, B and C show IP albumin injection markedly increased 24 hour urinary protein and

albumin from baseline. An average of 75% of the amount of albumin injected was recovered in the urine on days 2–5. This increase in albuminuria is consistent with previous results, which also showed no change in hematocrit or total plasma protein.[9] Glomerular filtration rate (GFR, ml/min/100 g) measured using 24-hour creatinine clearances, showed no significant measurable change between day 0 and 3 or 4 day 1=0.71±0.14, imaging day=0.68±0.12.

Acute Albumin Overload does not Correlate with Glomerular Sieving Alterations

This acute albumin overload model allowed us to determine whether elevated albumin excretion resulted from increased passage via the glomerular filtration barrier. Intravital two-photon microscopy was used to quantify GSCs on days 3 or 4, enabling us to evaluate GSC for rats with variable but elevated albuminuria levels. Each rat had an average of five surface glomeruli that were measured at two time points following Texas Red rat serum albumin (TR-RSA) infusion. Image collection did not start until at least 10 minutes post TR-RSA infusion to allow equilibration to occur. Figure 1D shows the GSC values on the y axis (overall mean of 0.0080±0.0013) and the corresponding 24-hour urine albumin values plotted on the x axis. Note, these values were also no different from GSCs for control MWF female rats (mean GSC of 0.0075±0.0029). If increased passage of albumin across the glomerular filtration barrier was the cause of albuminuria then one would expect that rats with the highest albumin excretion levels would have the highest GSC values. However, there was no correlation between the measured GSC for albumin and the 24-hour urinary albumin excretion. This result raised the possibility that a nonglomerular event was responsible for increased albumin excretion. The other well-studied mechanism that has been shown to contribute to elevated urinary albumin is an alteration in PTC uptake of filtered proteins.[2]

PT Albumin Reabsorption Decreased During Albumin Loading

Intravital microscopy was used to quantify tracer amounts of TR-RSA uptake by PTCs. Less TR-RSA appeared in the early S1 segment of the PTs (visible opening to glomerulus) in protein overload rats compared with control rats. An example of this is shown in Figure 2A where the control PT S1 had increased TR-RSA fluorescence than a PT S1 in the protein overloaded rat, images captured 20–30 min after TR-RSA infusion. To quantify TR-RSA uptake we used our established method that determines total PTC uptake without distinguishing between different PT segments, Figure 2B.[12] A box plot of these data gave a mean value of 3357±1339 total integrated fluorescence (TIF)/μm^2 for control and 1255±976 TIF/μm^2 for protein overload with a P value of 0.014. To further characterize uptake changes we focused on the robust endocytic activity of the S1 tubules, where a disproportionate amount of filtered proteins are reabsorbed. To determine S1 uptake the images showing PT with a clear glomerular-tubule lumen opening were quantified. An average of five glomeruli from each rat were identified that had an S1 and a total of 74 time points were analyzed for the protein
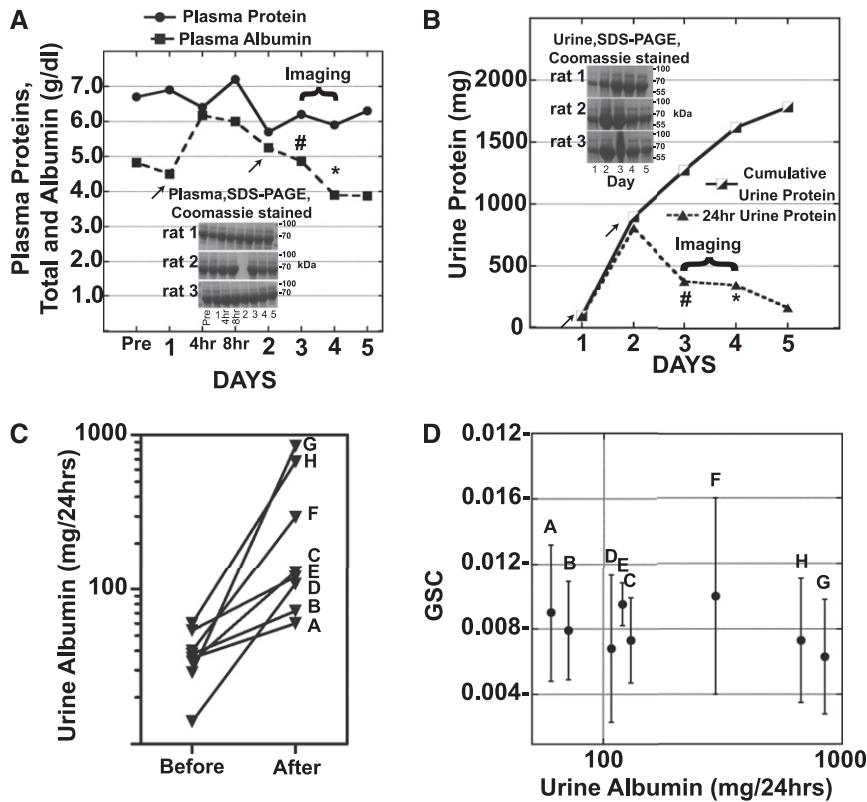
Figure 1. Acute albumin overload increases urine albumin but does not result in GSC increases. (A) Plasma SDS-PAGE Coomassie stained gels and the average (n=3, no plasma for rat 2 day 2 gel sample) plasma albumin and total protein in g/dl following two albumin injections (625 mg/100 g/day) on days 1 and 2 (arrows). Rats were evaluated by two-photon microscopy on days 3 or 4, 24 hours (#) or 48 hours (*) after the second injection. Note the rapid increase and return to baseline of serum albumin levels in this model. (B) Daily and cumulative 24 hour urine protein and Coomassie gels are shown. Blood was collected pre- and post-albumin injections and creatinine measured using the Jaffe method with the Pointe 180 QT Analyzer. Urine creatinine was measured and GFR calculated [UCR×UVOL (ml/min)/PCR]. GFR was unaffected by albumin injections. (C) 24 hour total urine albumin is presented for the eight MWF female rats before albumin injections and on the day of imaging after either 24 hours (F–H) or 48 hours (A–E) following the second injection. (D) A scatter plot is presented of the albumin GSC±SD and the 24 hour total urine albumin on the day of imaging. GSC was determined using two-photon microscopy as described earlier. Note the lack of correlation between GSC and urine albumin values.

overloaded rats. Three control rats were used and 36 time points were analyzed. We also normalized each S1 to its own glomerular capillary intensity to reduce variability and provide a more accurate assessment of the amount of filtered albumin reaching each individual S1 segment. These data are shown in Figure 2C. Plotting PTC-S1 intensity over time revealed a clear difference in TR-RSA uptake. Note, this change in TR-RSA uptake occurred even though the amount of albumin being filtered was constant (no change in GSC between control and protein overload animals) and total plasma protein and albumin were not significantly altered in this model on the days of our imaging study. Comparison of the line slopes with GraphPad Prism software showed a statistically significant difference in slopes, $P<0.0001$.

PT Cells have the Capacity to Increase Endogenous Albumin Reabsorption when Glomerular Albumin Permeability is Increased

To determine whether PTC could reabsorb additional endogenous albumin if rats were made albumin-deficient by excess albumin filtration, we developed and then utilized the human DT receptor expressing podocytes in MW Fromter rats (hDTR-Pod/SG rats) using previously published techniques.[11,15] Baseline serum albumin, 4.3±0.3 gm/dl, and 24-hour urinary albumin, 22.4±10.1 mg/24 hours were normal prior to DT treatment. Figure 3A shows a low-power view of untreated versus DT treated glomeruli at 5 days. At this point in time serum albumin was decreased to 2.560.4 gm/dl and 24-hour urinary albumin was increased at 148.3626.6 mg. Note the significant increase in TR-RSA taken up by the PT in the DT podocyte damaged kidneys. Exposure of these rats to DT resulted in dose- and time-dependent podocyte injury-dependent proteinuria with a corresponding increase in urinary albumin (Figure 3B), as previously reported.[11] This was associated with a marked increase in the GSC for albumin (0.017±0.006 versus 0.145±0.0067, $P<0.01$) on day 5 following 200 ng DT/kg. To examine how the PTs responded to this endogenous albumin exposure originating from leaky glomeruli in the setting of net albumin loss, intravital microscopy was used to quantify PTC TR-RSA uptake. Figure 3C shows quantitation of TR-RSA PT uptake in untreated and treated DT podocyte MWF rats. A box plot of these data gave a mean value of 1099±274 TIF/μm^2 for control and 3133±1648 TIF/μm^2 for DT treated rats with a P value <0.05. Note, given the large uptake observed in DT rats, some saturation of the detectors occurred, and so this increase likely represents an underestimate. These data support the fact that PTs have a large reserve capacity to reabsorb filtered albumin if needed.

FcRn Localization and Expression is not Impacted by Acute Protein Overload

Recent data have shown that the FcRn can bind albumin in a pH-sensitive manner with increased affinity at pHs at and below 6.[7,16,17] This enables it to be an ideal transcytotic receptor, attaching in the acidic environment of the endosome and releasing at the higher pH of the extracellular fluid. Reabsorbing and transcytosing filtered albumin may be fundamental to the long half-life of albumin (and IgG).[2,18] The hypothesis is that FcRn is
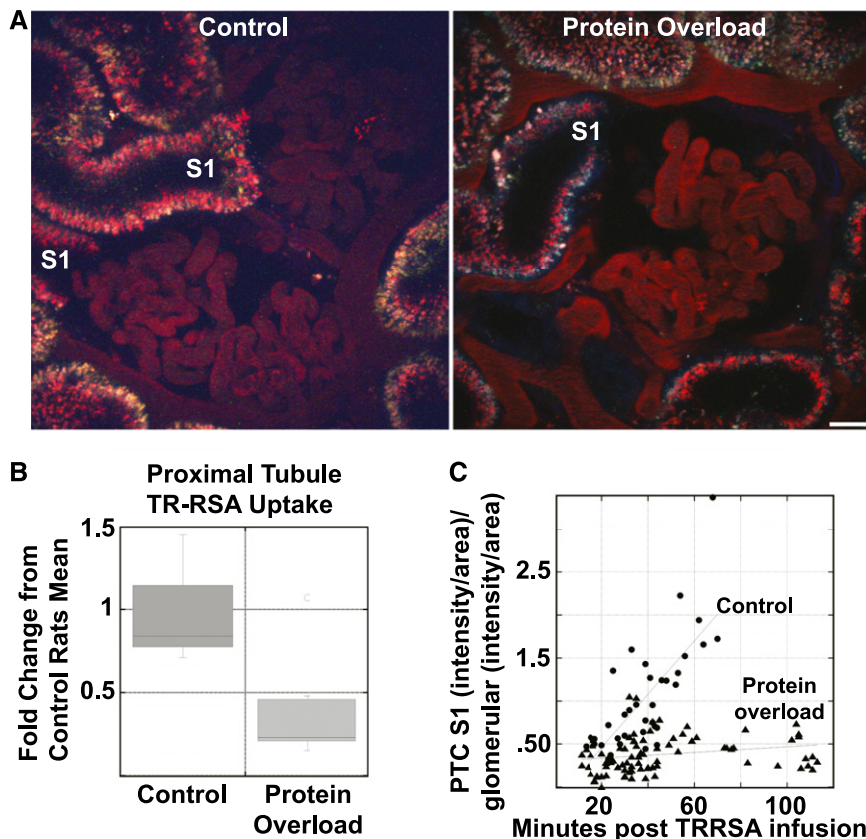
Figure 2. Acute albumin overload results in decreased PT uptake. (A) An intravital microscopy single time point image showing TR-RSA fluorescence in the S1 region of a control and protein overload animal, 20–30 min after TR-RSA infusion. Note the reduced uptake in the protein overload animal. Bar, 20 μm. (B) Box plot showing the quantification of TR-RSA uptake in all surface PTs of control (n=3 rats, 157 fields quantified) and protein overloaded (n=8 rats, 176 fields quantified) rats. This analysis showed a significant reduction in albumin uptake, P<0.01 (KaleidaGraph, Student's t-test). (C) Quantification of the TR-RSA uptake in only S1 PTC identified reduced uptake in the protein overload animals. Each data point represents an individual measurement from control (n=36 from three rats) or protein overload (n=83 from seven rats) S1 PT. The differences in the slopes of these lines was found to be significant, P<0.001, GraphPad Prism.

responsible for returning filtered albumin to the circulation whereas the megalin/cubilin transport system directs albumin toward degradation. Figure 4A documents the presence of FcRn by Western blot in rat kidney cortex and medulla. Note the upper FcRn band represents the glycoprotein modified form while the lower band is the immature form.[19,20] Further confirmation of FcRn's presence in both PT and CCD was achieved by RTPCR analysis of RNA isolated from micro-dissected rat tubules, Figure 4A. Figure 4B shows the location of FcRn using a polyclonal antibody directed against purified rat FcRn along with F-actin labeled with phalloidin to locate the brush border (BB). All immunofluorescent (IF) images are approximately 5 μm z projections and clearly show FcRn concentrated in the apical BB region of the PTC. Following acute protein overload (4B) no significant change in location was observed for FcRn. To address whether protein expression of FcRn or megalin was altered by

protein overload, Western blots were analyzed and no significant change in either protein was detected (data not shown). A recent report using the protein overload model similarly found no change in megalin levels.[21] Finally, to determine whether FcRn mRNA levels were altered by protein overload, qRT-PCR was performed on RNA isolated from kidney cortex and no significant difference was detected (Figure 4C).

Proteomic Analysis of Kidney Cortex Proteins Altered by Acute Protein Overload

To address more global changes occurring following protein overload, and to identify proteins and potential pathways impacting PTC albumin uptake, kidney outer cortex proteins were separated and analyzed. Individual proteins were separated by two-dimensional electrophoresis (2DE), quantified by image analysis and differentially expressed proteins identified by mass spectrometry. Table 1 lists the 35 significantly altered proteins identified with the abundance of 13 increased and 22 decreased. Notably albumin (+1.8-fold) showed the largest increase while calreticulin, a calcium-binding chaperone, the biggest decrease (−1.3-fold). Interestingly, one of the proteins increased was Disabled homolog 2, a clathrin-associated sorting protein required for clathrin-mediated endocytosis. Analysis of all 35 proteins using Ingenuity Pathway Analysis software identified two Upstream Regulators that were predicted to be inhibited. First, with an activation z-score of −2.169 and P value of 0.02 NFE2L2 (nuclear factor erythroid 2-related factor 2), a transcription activator important for the coordinated upregulation of genes in response to oxidative stress, was inhibited. Second, with an activation z-score of −1.664 and P value of 0.05 ANGPT2 (angiopoietin-2), a growth factor, was inhibited. This analysis also revealed a significant effect on three categories involved with ATP synthesis reflecting downregulation of five proteins involved in mitochondrial function (ATP5B, ATP5D, CHCHD6, HSPD1, VDAC1).

DISCUSSION

Intravital two-photon microscopy has enabled the investigation of cellular and subcellular events in tissues in live animals.[2,12,14,22] One of the main functions of the PTC is retrieval of filtered proteins and our studies, and other recent reports, support the importance of the PTC in regulating albumin excretion rate.[2]
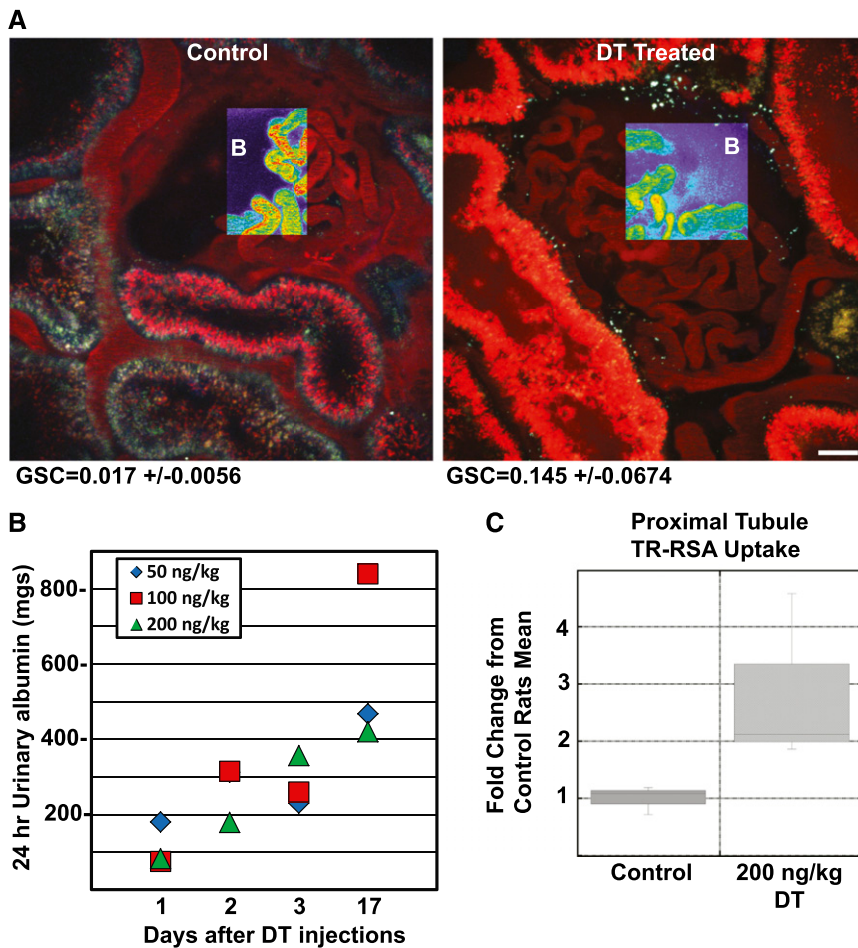
Figure 3. Damage to podocytes increases albuminuria and results in increased PT albumin uptake. (A) An intravital microscopy single time point image showing TR-RSA fluorescence in the glomerulus and adjacent tubules from a control and DT treated rat (day 5, 200 ng/kg). Note the increased amount of TR-RSA in the tubules following DT treatment. The pseudo-color overlays in a glomerular region clearly show the increase in leakage of the TR-RSA into Bowman's (B) space in the DT treated rat. This increased leakage correlates with the increased GSA calculated for DT treated rats (GSC=0.145±0.0674, n=3) compared with control untreated rats (GSC=0.017±0.0056, n=3). Bar, 20 μm. (B) DT dose and time response shows a linear increase with 24 hour albuminuria. C. Box plot showing the quantification of TR-RSA uptake in all surface PTs, of control (n=3 rats, 101 fields quantified) and DT treated (n=3 rats, 106 fields quantified) rats. This analysis showed a significant increase in albumin uptake, P=0.05 (Student's t-test one-tailed equal variance).

Further, the recent identification of an albumin receptor, FcRn, which is present in the kidney and mediates transcytosis in PT cells, provides a mechanism for returning filtered albumin to the circulation.[2,4]

The present study had three main objectives. First, to determine whether an acute systemic albumin load, achieved by two intraperitoneal albumin injections, resulting in increased albumin excretion, causes detectably increased glomerular filtration of albumin. Second, to establish how increased albuminuria from two distinct models impacts PTC albumin uptake. Third, to begin identification of pathways and/or proteins contributing to the observed proteinuria that may participate in regulation of PT

protein retrieval. Several studies have utilized albumin overload models in mice, rats, and cultured cells and distinct differences between rat strains have been demonstrated.[9,10,21,23] The question of whether persistent proteinuria can be detrimental to kidney function remains controversial.[24] Several studies have documented glomerular structural changes including podocyte flattening and foot process fusion,[9,25,26] however normal glomeruli were also observed in these same studies. Other animal studies suggested that the protein uptake pathway in PTC may become saturated and that an increase in PTC lysosomal activity may occur.[21] In vitro cell studies also support changes taking place in PTC with protein overload.[26–28] Finally, a study in Wistar rats using three albumin injections, versus two as in our study, showed no change in the glomerular size selectivity.[29]

For the present study, we chose an acute albumin overload model using two albumin injections in normal healthy animals. In this model serum protein levels were maintained, but not increased. Our results showed that neither GFRs nor the GSCs for albumin were altered under the conditions used. Plasma albumin did increase modestly but returned to normal within 24 hours of the second RSA injection and prior to our quantification of GSC. Together, these data support that a relatively constant amount of albumin is being delivered to the tubules. Using the data generated from our studies we did mass balance calculations. As is shown in Figure 5, utilizing GSC, PT uptake, serum albumin, and GFR, urine albumin could be calculated and was in close agreement with the observed amount. With a GSC of approximately 0.08, and GFR of 0.7 ml/100 g body weight, a 200 g rat would filter approximately 725 mg albumin/day (Figure 5). We observed that under these conditions both S1 and cortical PTC albumin uptake were markedly reduced in response to an acute exposure to exogenous albumin. This result strongly suggests that in the setting of increased total body albumin load PT reclamation of albumin can be down-regulated. A mass balance summary of these changes is shown in Figure 5. The sensor(s) responsible for regulating albumin reabsorption and transcytosis remains to be determined. Possibilities include cellular or hormonal regulation of transporters and possibilities include physiochemical alterations on the basolateral aspect of the cell related to peritubular capillary and interstitial albumin concentrations. These data also indicate that the long-held assumption that increased albuminuria following albumin loading was due to an
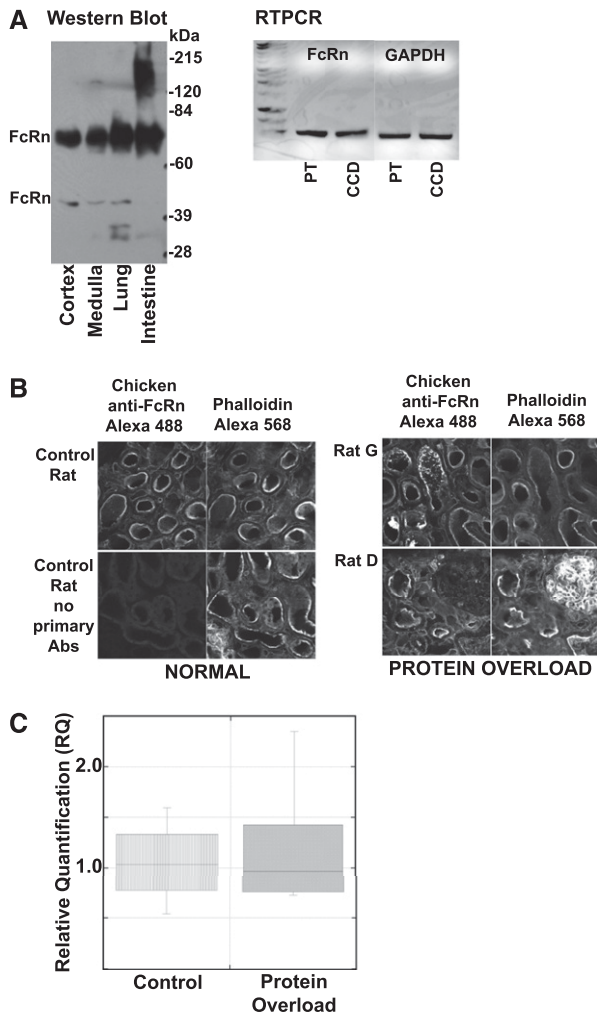
Figure 4. FcRn location and levels do not correlate with protein overload changes. (A) Western blot of rat tissue (left panel) (kidney cortex, kidney medulla, lung and intestine) with equal amounts of proteins loaded on gel show FcRn is present in both kidney regions. Note, the upper FcRn band corresponds to the mature glycosylated form while the lower band is the immature form.[19,20] In the right panel, RNA from micro-dissected PT and CCD, kindly provided by Dr. Lisa Satlin, were analyzed using RTPCR for FcRn and GAPDH. This also supports the presence of FcRn in both tubule segments. (B) Immunofluorescent localization of FcRn in control and protein overload (rats G and D) rat kidney cortex. Each section was labeled with the chicken anti FcRn Ab and phalloidin. Sequential laser excitation of each dye prevented any fluorescent crosstalk. Presented images consist of <5 μm z projections showing the same field and planes for both labels. Note that no significant difference was observed following protein overload. (C) FcRn qPCR was performed on RNA isolated from control (n=4) and protein overloaded rats (n=6). Box plot of the RQ results showed no significant difference in expression levels for FcRn, control mean 1.05±0.43 and protein overload mean 1.20±0.63. GAPDH, glyceraldehyde-3-phosphate dehydrogenase; RQ, relative quantification.

alteration in glomerular filtration of albumin was not correct, and that PT reabsorption was the determinant of urinary albumin excretion.

To further test the hypothesis that PTs can regulate albumin reabsorption, we used a model that would likely saturate the PTC capacity to reabsorb albumin and thereby result in net body albumin depletion. This experimental design would address whether PTCs have the capacity to reabsorb additional albumin in the setting of albumin depletion if presented in the glomerular filtrate, *i.e.*, no exogenous albumin is delivered to these animals. To do this we utilized the hDTR-Pod/SG rat model, developed for MWF rats, which in the presence of DT specifically injures podocytes, resulting in a dose- and time-dependent increase in albumin excretion rate.[11] Our data extend the previous work by directly showing dose- and time-dependent increases in GSC for albumin and depletion of serum albumin as a result. Given the increase in GSC with DT treatment, a 10-fold increase in filtered albumin would be calculated. An accurate quantitation of filtered albumin is complicated by variable degrees of tubule blockage that occur in this model. However, under these conditions the PTs showed a remarkable capacity to increase albumin uptake (Figure 3C), with a 2.85-fold increase over control. A complete mass balance for the DT model will require further investigation, with some limitations given the large albumin uptake that can rapidly saturate fluorescent detectors, and potential for tubule blockage.

Taken together these data have important clinical implications, as they indicate, for the first time, that PTC uptake of albumin is regulated, with the capacity to either decrease or increase albumin reabsorption. The regulation of PTC albumin uptake has many clinical implications and may involve changes in albumin receptors and/or other regulatory mechanisms that enable these cells to alter their albumin reclamation depending upon serum albumin levels. Therefore, a complete understanding of this important process should be the target of future investigations.

Reduced PTC protein uptake has been shown to occur in megalin/cubilin knockout animals and in *in vitro* cell studies that have targeted this well-studied multi-ligand receptor.[30–37] However, in all of these studies albuminuria was not markedly increased, thus supporting recent evidence for other mechanisms having an active role in albumin retrieval occurring in PTCs. FcRn, the only albumin transcytotic receptor yet identified, is concentrated in the apical region of the PTCs as shown in Figure 4B. Western blots for both megalin and FcRn amount and distribution were not detectably altered following protein overload as assessed by Western blot or immunolocalization studies. However, both these proteins have multiple regulatory pathways, *i.e.*, phosphorylation, glycosylation, which have been shown to impact their function and may be occurring during the protein overload.[38–45] A regulatory switch to reduce albumin uptake following acute albumin intake would be advantageous for maintaining a healthy kidney and overall homeostasis. Similarly, a mechanism to increase protein uptake following a transient increase in GSC for albumin would serve to maintain serum albumin levels.
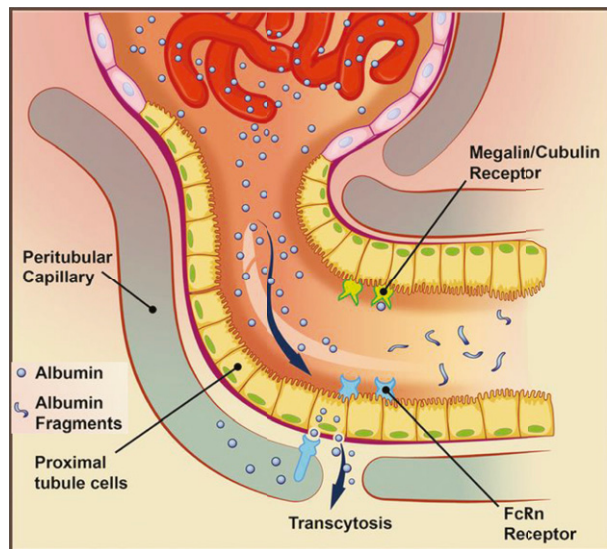
Previous studies that have investigated albuminuria models have not used intravital microscopy. This method enables one to follow the dynamic filtration and uptake of fluorophore

Table 1. Kidney cortex proteins altered by protein overload

Gene ID Protein ID	P Value	Fold Change	Description (UniProt)
Albu Serum Albumin	<0.001	+1.8	The main protein of plasma, has a good binding capacity for water, Ca^{2+}, Na^+, K^+, fatty acids, hormones, bilirubin and drugs. Its main function is the regulation of the colloidal osmotic pressure of blood. Major zinc transporter in plasma, typically binds about 80% of all plasma zinc.
Calr Calreticulin	<0.01	−1.3	Calcium-binding chaperone that promotes folding, oligomeric assembly and quality control in the ER via the calreticulin/calnexin cycle. This lectin interacts transiently with almost all of the monoglucosylated glycoproteins that are synthesized in the ER.
Dab2 Disabled homolog 2	>0.02	+1.2	Adapter protein that functions as clathrin-associated sorting protein (CLASP) required for clathrin-mediated endocytosis of selected cargo proteins. Can bind and assemble clathrin, and binds simultaneously to phosphatidylinositol-4,5-bisphosphate (PtdIns(4,5)P2) and cargos containing non-phosphorylated NPXY internalization motifs, such as the LDL receptor, to recruit them to clathrin-coated pits.
Dlat Dihydrolipoyllysine-residue acetyltransferase component of pyruvate dehydrogenase complex	>0.02	+1.2	The pyruvate dehydrogenase complex catalyzes the overall conversion of pyruvate to acetyl-CoA and CO_2, and thereby links the glycolytic pathway to the tricarboxylic cycle.
Tpm3 Tropomyosin alpha-3 chain	0.004	+1.2	Binds to actin filaments in muscle and non-muscle cells. In non-muscle cells is implicated in stabilizing cytoskeleton actin filaments.
Prdx2 Peroxiredoxin-2	0.05	+1.2	Involved in redox regulation of the cell. Reduces peroxides with reducing equivalents provided through the thioredoxin system. It is not able to receive electrons from glutaredoxin. May play an important role in eliminating peroxides generated during metabolism. Might participate in the signaling cascades of growth factors and tumor necrosis factor-alpha by regulating the intracellular concentrations of H_2O_2.
Gm2a Ganglioside GM2 activator	0.05	+1.2	The large binding pocket can accommodate several single chain phospholipids and fatty acids; GM2A also exhibits some calcium-independent phospholipase activity.
Ssbp1 Single-stranded DNA-binding protein	>0.02	+1.2	This protein binds preferentially and cooperatively to ss-DNA. Probably involved in mitochondrial DNA replication.
Asrgl1 Isoaspartyl peptidase/L-asparaginase	>0.02	+1.2	Has both L-asparaginase and beta-aspartyl peptidase activity. Is highly active with L-Asp beta-methyl ester.
Acot13 Acyl-coenzyme A thioesterase 13	>0.02	+1.2	Acyl-CoA thioesterases are a group of enzymes that catalyze the hydrolysis of acyl-CoAs to the free fatty acid and coenzyme A (CoASH), providing the potential to regulate intracellular levels of acyl-CoAs, free fatty acids and CoASH.
Fkbp2 Peptidyl-prolyl cis-trans isomerase	>0.02	+1.2	PPIases accelerate the folding of proteins. It catalyzes the cis-trans isomerization of proline imidic peptide bonds in oligopeptides.
Lyz1 Lysozyme C-1	>0.02	+1.2	Lysozymes have primarily a bacteriolytic function; those in tissues and body fluids are associated with the monocyte-macrophage system and enhance the activity of immunoagents. In the intestine they may also have a digestive function.
Btf3 Basic transcription factor 3	0.01	+1.2	When associated with NACA, prevents inappropriate targeting of non-secretory polypeptides to the endoplasmic reticulum (ER). Binds to nascent polypeptide chains as they emerge from the ribosome and blocks their interaction with the signal recognition particle (SRP), which normally targets nascent secretory peptides to the ER. BTF3 is also a general transcription factor that can form a stable complex with RNA polymerase II. Required for the initiation of transcription.
Cfl2 Cofilin 2	0.01	+1.2	Controls reversibly actin polymerization and depolymerization in a pH-sensitive manner. It has the ability to bind G- and F-actin in a 1:1 ratio of cofilin to actin. It is the major component of intranuclear and cytoplasmic actin rods.
Dld Dihydrolipoyl dehydrogenase	>0.01	−1.2	Lipoamide dehydrogenase is a component of the glycine cleavage system as well as of the alpha-ketoacid dehydrogenase complexes. Involved in the hyperactivation of spermatozoa during capacitation and in the spermatozoal acrosome reaction.

Table 1. Continued

Gene ID Protein ID	P Value	Fold Change	Description (UniProt)
Aldh8a1 Aldehyde dehydrogenase family 8 member A1	>0.01	−1.2	Converts 9-cis-retinal to 9-cis-retinoic acid. Has lower activity toward 13-cis-retinal. Has much lower activity toward all-trans-retinal. Has highest activity with benzaldehyde and decanal (in vitro). Highly expressed in adult kidney and liver.
Oxct1 Succinyl-CoA:3-ketoacid coenzyme A transferase 1	>0.01	−1.2	Key enzyme for ketone body catabolism. Transfers the CoA moiety from succinate to acetoacetate. Formation of the enzyme-CoA intermediate proceeds via an unstable anhydride species formed between the carboxylate groups of the enzyme and substrate.
Glud1 Glutamate dehydrogenase 1	>0.01	−1.2	Mitochondrial glutamate dehydrogenase that converts L-glutamate into alpha-ketoglutarate. Plays a key role in glutamine anaplerosis by producing alpha-ketoglutarate, an important intermediate in the tricarboxylic acid cycle.
Calb1 Calbindin	<0.01	−1.2	Buffers cytosolic calcium. May stimulate a membrane Ca^{2+}-ATPase and a 3′,5′-cyclic nucleotide phosphodiesterase.
Psma5 Proteasome subunit alpha type-5	<0.01	−1.2	The proteasome is a multicatalytic proteinase complex which is characterized by its ability to cleave peptides with Arg, Phe, Tyr, Leu, and Glu adjacent to the leaving group at neutral or slightly basic pH. The proteasome has an ATP-dependent proteolytic activity.
Atp5d ATP synthase subunit delta	0.02	−1.2	Mitochondrial membrane ATP synthase (F_1F_0 ATP synthase or Complex V) produces ATP from ADP in the presence of a proton gradient across the membrane which is generated by electron transport complexes of the respiratory chain.
Myl6 Myosin light polypeptide 6	0.02	−1.2	Regulatory light chain of myosin. Does not bind calcium.
Atp6v1b2 V-type proton ATPase subunit B, brain isoform	0.04	−1.1	Non-catalytic subunit of the peripheral V1 complex of vacuolar ATPase. V-ATPase is responsible for acidifying a variety of intracellular compartments in eukaryotic cells.
Hspd1 60 kDa heat shock protein	0.04	−1.1	Implicated in mitochondrial protein import and macromolecular assembly. May facilitate the correct folding of imported proteins. May also prevent misfolding and promote the refolding and proper assembly of unfolded polypeptides generated under stress conditions in the mitochondrial matrix.
Pdia3 Protein disulfide-isomerase A3	0.04	−1.1	Catalyzes the rearrangement of –S–S– bonds in proteins.
Pepd Xaa-Pro dipeptidase	0.04	−1.1	Splits dipeptides with a prolyl or hydroxyprolyl residue in the C-terminal position. Plays an important role in collagen metabolism because of the high level of iminoacids in collagen.
Chdh Choline dehydrogenase	0.04	−1.1	Choline + acceptor = betaine aldehyde + reduced acceptor.
Cat Catalase	0.04	−1.1	Occurs in almost all aerobically respiring organisms and serves to protect cells from the toxic effects of hydrogen peroxide. Promotes growth of cells.
Pyroxd2 Pyridine nucleotide-disulfide oxidoreductase domain-containing protein 2	0.04	−1.1	Probable oxidoreductase.
Atp5b ATP synthase subunit beta	<0.03	−1.1	Mitochondrial membrane ATP synthase (F_1F_0 ATP synthase or Complex V) produces ATP from ADP in the presence of a proton gradient across the membrane which is generated by electron transport complexes of the respiratory chain.
Pdia6 Protein disulfide-isomerase A6	<0.03	−1.1	May function as a chaperone that inhibits aggregation of misfolded proteins.
Chchd6 Coiled-coil-helix-coiled-coil-helix domain-containing protein 6	<0.01	−1.1	Required for maintaining mitochondrial crista morphology, ATP production and oxygen consumption.
Tst Thiosulfate sulfurtransferase	<0.01	−1.1	Together with MRPL18, acts as a mitochondrial import factor for the cytosolic 5S rRNA.
Hadh Hydroxyacyl-coenzyme A dehydrogenase	<0.01	−1.1	Plays an essential role in the mitochondrial beta-oxidation of short chain fatty acids. Exerts its highest activity toward 3-hydroxybutyryl-CoA.
Vdac1 Voltage-dependent anion-selective channel protein 1	<0.01	−1.1	Forms a channel through the mitochondrial outer membrane and also the plasma membrane. The channel at the outer mitochondrial membrane allows diffusion of small hydrophilic molecules; in the plasma membrane it is involved in cell volume regulation and apoptosis.

	GFR (ml/min)	Serum Alb (mg/ml)	GSC$_A$	Albumin Filtered (mg/24hr)	PT Uptake (%)	Urine Alb Calculated (mg/24hr)	Urine Alb Observed (mg/24hr)
Control	1.4	45	0.008	725	95	X	38
Protein Overload	1.4	45	0.008	725	37	457	329

Figure 5. Mass balance of albumin filtration, PT reabsorption and urinary excretion, 200 g rat. Albumin filtered was calculated by using mean values from this study for GFR, serum albumin and GSC for albumin. Thus calculated 24 hour urinary albumin was determined by the following equation: GFR×1440 minutes×serum albumin (mg/ml) ×GSC×(1−%PT uptake). %PT uptake for control was calculated by dividing observed 24 hour albumin by calculated albumin filtered×100. %PT uptake for PO was calculated from mean data in Figure 2B and is very close to observed 24 hour urinary albumin. Note the ability of the PT to down-regulate albumin reabsorption.

conjugated albumin in surface glomeruli and tubules. The dynamics of deeper glomeruli and tubules not visible by two-photon imaging can't be directly addressed with this method, and this remains a limitation. Because FcRn is the only known transcytotic albumin receptor, and rat FcRn binds bovine albumin with reduced affinity, we utilized rat albumin for these studies.[4,7,16,46] Species differences in albumin and IgG binding to FcRn are well documented and may contribute to some of the variability reported in protein overload studies. The binding affinity for megalin/cubilin for different albumins has yet to be determined but this receptor has been shown to only target albumin to lysosomes.[6] Consequently, retrieval of albumin and return to the circulation would be expected to require involvement of FcRn. This is supported by studies in knockout mice and more recently by some elegant studies using transgenic mice and rat models by the Moeller group.[4,46] To identify possible pathways that could be participating in the reduced PT albumin uptake, quantitative two-dimensional gel electrophoresis (2DE) combined with mass spectrometry and pathway analysis was conducted on kidney cortex proteins from control and protein overload rats. The largest increase (1.8×) was observed for albumin. The other notable protein increased was Dab2 (+1.2-fold) which binds to megalin and is present in the PTC coated pits.[31,47] Interestingly, a recent study using human PTCs to identify a link

between Dab2 and PKB/Akt partners showed a reduction in Dab2-reduced albumin endocytosis. Yet an increase in Dab2 and PKB/Akt appears to be protective.[48] Further investigation is needed to define how Dab2 is acting in this model. The largest fold decrease (−1.3) was observed for calreticulin, which along with calnexin is part of the endoplasmic reticulum (ER) chaperone system.[49] These lectins associate with most glycoproteins being involved with folding, quality control and degradation. Interestingly, there is evidence that calnexin binds glycated albumin.[50] Albumin was also upregulated and whether this relates to increases in tubular fluid, interstitial or cellular albumin was not determined. Five proteins that decreased in abundance (ATP5B, ATP5D, CHCHD6, HSPD1, VDAC1) are involved in synthesis of ATP, which may indicate ATP levels or turnover are reduced; this has been shown to regulate cytoskeletal events and even reduce endocytosis in cells.[51]

Analysis of all protein changes using Ingenuity IPA software revealed that two potentially important upstream regulators were predicted to be inhibited. First, NFE2L2 encodes the protein Nrf2, which is part of the cytoprotective Keap1-Nrf2 pathway.[52] Normally repressed by its association with Keap1-Cul3 complex in the cytoplasm, Nrf2 migrates to the nucleus upon stress induction and binds to specific response elements inducing expression of target genes to detoxify, provide oxidant protection, and other stress response mediators. Multiple studies have documented that induction of Nrf2 is protective for the kidney in CKD, diabetic nephropathy, renal fibrosis, ischemia and other insults.[52] The fact that this was inhibited suggests the acute overload model does not induce stress nor needs the stress response elements increased, thus preventing an over-reaction to this acute protein load. The second upstream regulator inhibited was ANGPT2. This gene encodes Angiopoietin-2 (Ang2), which is an antagonist of the Tie2 receptor and when bound causes vascular destabilization and leakage.[53] Some evidence suggests that it can also function as an agonist, depending upon concentration.[54] Its precise role in kidney function is unclear as one study showed no protection in a mouse septic model while higher Ang2 levels were a good predictor of increased mortality in kidney transplant recipients.[53,55] The proteomic results support the concept that the kidney has developed an intricate means of responding to acute protein overloads to maintain normal function and reduce injury. Further research will be needed to confirm the biologic significance of the proteomic changes observed.

In summary, we have addressed the regulation of PT albumin uptake using two animal models, one that results in an acute exogenous albumin overload and another which causes podocyte damage and sustained endogenous albuminuria. The acute albumin overload did not cause detectably increased glomerular filtration of albumin but did reduce albumin uptake in the S1 and all cortical PTs. This lack of reabsorption of filtered albumin occurred even though the PTC has additional capacity to increase albumin reabsorption when called upon to do so. This was confirmed by using the DTr podocyte expressing rat model, which resulted in increased GSC and markedly increased PT albumin uptake. Proteomic analysis suggests that complex and protective cellular responses occur during an acute protein overload that may be designed to maintain the albumin milieu and diminish detrimental effects of albuminuria on the kidney. This has important clinical implications in the therapeutic approach to albuminuria.

MATERIALS AND METHODS

Animals

Female MWF rats (9–12 weeks old) were derived from a colony generously provided by Dr. Roland Blantz (University of California—San Francisco, San Diego, CA). All rats were given water and food *ad libitum* throughout the study. Rats were administered two IP injections 24 hours apart of rat albumin (A6272, 625 mg/100 g/day; Sigma-Aldrich, St. Louis, MO) with imaging occurring between 24 and 48 hours after the second injection. Plasma and urine albumin, plasma total protein and urine total protein (24 hour collection in metabolic cages) were quantified using a bromocresol green dye-binding procedure, Biuret reagent set, and a Pyrogallol Red method, respectively, as recommended for the Pointe 180 QT Analyzer (Pointe Scientific Canton, MI). All experiments followed the NIH Guide for the Care and Use of Laboratory Animals guidelines and were approved by the Animal Care and Use Committee at the Indiana University School of Medicine or Icahn School of Medicine at Mount Sinai (for studies in micro-dissected tubules of SD rats).

hDTR-Pod/SG rats were produced in the Wiggins laboratory at the University of Michigan. MWF rats with superficial glomeruli were provided by the Molitoris Laboratory at Indiana University. They were crossed with human diphtheria toxin receptor (hDTR) transgenic Fischer344 rats in which DT can be injected to deplete podocytes in a dose- and time-dependent manner.[11] In hDTR rats the transgene is driven by the human podocin promoter, which results in podocyte-specific gene expression as previously described.[11,15] After each step the offspring were genotyped to select for the hDTR transgene and a kidney biopsy was performed to select for superficial glomeruli. After five generations of selection rats were then inbred to select for homozygosity of the hDTR transgene using the Q-PCR TaqMan assay to measure transgene copy number. This novel rat line containing superficial glomeruli and homozygous for the hDTR transgene in podocytes has been maintained since 2007 as a breeding colony and are designated hDTR-Pod/SG rats.

Fluorescent Albumin Synthesis

Rat serum albumin (fraction V; Sigma-Aldrich) was conjugated to Texas Red sulfonyl chloride according to the manufacturer's instructions (Invitrogen, Carlsbad, CA) to give a stoichiometric ratio of approximately 4:1 mol dye: albumin. Conjugation was confirmed as described previously using absorbance measurements and dialyzed extensively using 50 kDa dialysis membrane (Float-A-lyzer, Spectrum Labs) to remove small fragments and any free dye prior to infusion.

Two-Photon Microscopy

Imaging was conducted using an Olympus FV1000 microscope adapted for two-photon microscopy with high-sensitivity gallium arsenide nondescanned 12-bit detectors with animal preparations, as described elsewhere.[3,12] Animals were anesthetized with sodium pentobarbital (50 mg/ml). A jugular venous line was used to introduce fluorescent albumin. As previously described, animal body temperature, saline bath temperature in dish and heart rate and blood pressure (90 mmHg avg) were measured using LabChart 6 (AD Instruments, Colorado Springs, CO).[12] All rats had normal body temperature, blood pressure and hydration was maintained by saline infusion.

Immunofluorescence of Rat Kidney Sections

Rat kidneys were perfusion-fixed via the abdominal aorta with 4% paraformaldehyde in PBS, pH 7.4. After perfusion fixation, the kidneys were trimmed and immersion fixed at 4 °C until sectioning. Sections (100 μm thick) were obtained using a Vibratome. For immunolabeling, the sections were rinsed with PBS, and permeabilized with 1% SDS for 3 minutes. After detergent treatment, the tissue sections were rinsed with PBS and placed in primary antibody in 0.5% fish skin gelatin in PBS for an overnight incubation. Following PBS washes secondary antibodies conjugated to their respective fluorophores were incubated with sections for 2 hours, followed by an overnight rinse with PBS and mounting with ProLong Gold (Molecular Probes). Images were collected using the Olympus FV1000 scanning confocal microscope. Sequential laser excitation of the three fluorophores eliminated crosstalk of fluorescent signals.

Western Blot Analysis

SDS-PAGE was carried out using Bio-Rad Criterion gels (Hercules, CA) or Lonza Gold precast gels (Thermo Fisher Scientific, Hanover Park, IL). PageRuler Plus Prestained molecular mass standards 10–250 kDa from Thermo Fisher Scientific were used. For immunoblotting, samples were resolved by SDS-PAGE and transferred by electroblotting to EMD Millipore polyvinyl difluoride (Bedford, MA). Pierce's ECL kit was used for detection. Monoclonal antibody 1G3 (ATCC CRL-2434) was the primary antibody used for this analysis and has been shown to recognize the FcRn heavy chain.

Two-Dimensional Gel Electrophoresis, Image Analysis, and Mass Spectrometry

A modification of our previously published procedure was used for these studies.[56] Briefly, frozen pulverized cortex tissue from protein overload and control rats was solubilized in 8 M urea, 4% CHAPS, 100 mM DTT, 40 mM Tris-Base pH 9.5, 0.4% carrier ampholytes (3–10). 200 μg of protein was loaded onto IPG strips (11 cm, nonlinear pH 3–10, Bio-Rad, Hercules, CA) using overnight passive rehydration at room temperature. Isoelectric focusing (IEF) was performed using the Protean IEF cell for 45,000 V-hours. IPG strips were then run on second dimension SDS-PAGE Criterion gels, stained with a modified colloidal Coomassie Blue G-250,[57] and imaged using a Bio-Rad ChemiDoc MP system. The resulting 16-bit Tiff images were analyzed using Progenesis SameSpots™ (v3.0, Nonlinear Dynamics, Durham, NC) and its embedded ANOVA analytic software as previously described.[56] For mass spectrometry, protein spots showing significant changes with protein overload were manually excised and analyzed as previously described.[56,58] The acquired mass spectral data were searched against the International Protein Index rat database using SEQUEST, validated using PeptideProphet and ProteinProphet in the Trans-Proteomic Pipeline[59,60] and only those proteins with greater than 90% confidence were considered identifications. Protein functions were derived from either the EntrezGene or UniProtKB/Swiss-Prot entries provided at GeneCards.

RNA Isolation and Quantification

Kidney tubules were isolated as previously described with 7.5 mm of PT and 3.5 mm of CCD used.[61] Kidney cortex from protein overload and control rats was dissected on ice in PBS and rapidly frozen in liquid nitrogen. Tissue was pulverized using the Cell-Crusher (Portland, OR) in liquid nitrogen and stored at −80°C until needed. Pulverized tissue was homogenized in TRI reagent (Sigma-Aldrich) according to the manufacturer's instructions. Yield and purity was verified by absorbance and gel analysis. RNA was stored in RNase-free water at –80°C.

Real-Time PCR

RNA was isolated using TRI Reagent (Sigma-Aldrich) according to their protocol. cDNA was made using the High Capacity cDNA Reverse Transcription Kit from Invitrogen/Applied Biosystems. cDNA was measured and equal amounts were run in the Applied Biosystems 7500 Real-Time PCR systems (Applied Biosystems). The primers for the qPCR were FAM-labeled specific for Fcgrt gene and VIC-labeled endogenous control for glyceraldehyde-3-phosphate dehydrogenase. The cycle number at which the amplification plot crosses the threshold was calculated (CT), and the $\Delta\Delta$CT method was used to calculate the relative quantification, which revealed no significant change in FcRn expression in the protein overload samples.

Quantitation of GSC and PTC Albumin Uptake

The GSCs were determined using our previously published method.[3] Briefly, z stack images of the glomerulus before TR-RSA infusion are collected to enable background fluorescent levels of the Bowman's space and glomerular capillaries to be quantified. These values are subtracted from the same region following the fluorescent albumin infusion. Quantification of intensity values was performed using Metamorph (Molecular Devices) or ImageJ. Graphing and statistical analysis was performed using Microsoft Excel (Redmond, CA), KaleidaGraph (Synergy Software Reading, PA) and GraphPad Prism 5 (La Jolla, CA).

PTC albumin uptake was quantified in two ways. First, all PTC were analyzed using our published procedure.[12] This involves generation of a background image, by using a 32×32 median filter, which is subtracted from the original image. Endosomes are selected by thresholding and total integrated fluorescence (TIF) was recorded per μm^2 of PT. A box plot was used to graph the TIF/μm^2 for comparing TR-RSA uptake. The Student's t-test gave a P value of 0.014. The DT treated and control rats were quantified using the same method and a P value of 0.05 was obtained. In both cases the box plots were normalized to the mean of the control rats.

The second quantitative analysis performed for the protein overload rats was restricted to early S1 segments defined by having a direct glomerular opening in the fluorescent images. For this analysis the following steps were performed in ImageJ:

1. From a TR-RSA post-infusion image file, three image planes (1 μm z steps) <25 μm from the kidney surface were selected and a SUM Z projection created.

2. A pre-infusion image file of the same S1 tubule was opened and a SUM Z projection of similar planes was created.

3. Magnify the pre-SUM image and use the Freehand selection tool to draw Region of Interest (ROI) around the S1 tubule being careful to avoid other cells and regions. Add this ROI to the ROI manager and then analyze selecting for: Area, Mean gray value, and Raw Integrated density. The Mean gray value of the pre-image is subtracted from the post-infusion SUM image (created as done for the pre-SUM image) by using the Process>Math>Subtract function in ImageJ then the ROI is analyzed as above.

Given the observed variability in fluorescence signal between animals and within kidney glomeruli capillaries a glomerular normalization was included as follows:

1. Using the same pre- and post-SUM images used for S1 uptake measurements the glomerular raw intensity is defined by using the ROI tool and threshold to accurately measure the glomerular capillary values. The pre-mean gray value is subtracted from the post-SUM image as was done for the S1 analysis. The final calculation is the following:

S1 Raw integrated density/area (BKG subtracted)/
Glomerulus Raw integrated density/area (BKG subtracted).

Statistical Analysis

All data are presented as mean±SD. Data were compared using unpaired Student's t-test. Differences were considered

statistically significant with $P<0.05$. Analysis was performed using GraphPad Prism Version 5.0 software (GraphPad Software Inc., La Jolla, CA), KaleidaGraph 4.0 (Synergy Software, Reading, PA) and Microsoft Excel. Specific *n* values for each figure are presented in the figure legends.

ACKNOWLEDGMENTS

DISCLOSURES

None.

REFERENCES

1. Roscioni SS, Lambers Heerspink HJ, de Zeeuw D: Microalbuminuria: target for renoprotective therapy PRO. *Kidney Int* 86: 40–49, 2014
2. Dickson LE, Wagner MC, Sandoval RM, Molitoris BA: The proximal tubule and albuminuria: really! *J Am Soc Nephrol* 25: 443–453, 2014
3. Sandoval RM, Wagner MC, Patel M, Campos-Bilderback SB, Rhodes GJ, Wang E, Wean SE, Clendenon SS, Molitoris BA: Multiple factors influence glomerular albumin permeability in rats. *J Am Soc Nephrol* 23: 447–457, 2012
4. Tenten V, Menzel S, Kunter U, Sicking E-M, van Roeyen CRC, Sanden SK, Kaldenbach M, Boor P, Fuss A, Uhlig S, Lanzmich R, Willemsen B, Dijkman H, Grepl M, Wild K, Kriz W, Smeets B, Floege J, Moeller MJ: Albumin is recycled from the primary urine by tubular transcytosis. *J Am Soc Nephrol* 24: 1966–1980, 2013
5. Birn H, Christensen EI, Nielsen S: Kinetics of endocytosis in renal proximal tubule studied with ruthenium red as membrane marker. *Am J Physiol* 264: F239–F250, 1993
6. Christensen EI, Birn H: Megalin and cubilin: synergistic endocytic receptors in renal proximal tubule. *Am J Physiol Renal Physiol* 280: F562–F573, 2001
7. Anderson CL, Chaudhury C, Kim J, Bronson CL, Wani MA, Mohanty S: Perspective— FcRn transports albumin: relevance to immunology and medicine. *Trends Immunol* 27: 343–348, 2006
8. Schaeffer C, Creatore A, Rampoldi L: Protein trafficking defects in inherited kidney diseases. *Nephrol Dial Transplant* 29[Suppl 4]: iv33–iv44, 2014
9. Weening JJ, Van Guldener C, Daha MR, Klar N, van der Wal A, Prins FA: The pathophysiology of protein-overload proteinuria. *Am J Pathol* 129: 64–73, 1987
10. Yoshida S, Nagase M, Shibata S, Fujita T: Podocyte injury induced by albumin overload in vivo and in vitro: involvement of TGF-beta and p38 MAPK. *Nephron Exp Nephrol* 108: e57–e68, 2008
11. Wharram BL, Goyal M, Wiggins JE, Sanden SK, Hussain S, Filipiak WE, Saunders TL, Dysko RC, Kohno K, Holzman LB, Wiggins RC: Podocyte depletion causes glomerulosclerosis: diphtheria toxin-induced podocyte depletion in rats expressing human diphtheria toxin receptor transgene. *J Am Soc Nephrol* 16: 2941–2952, 2005
12. Sandoval RM, Molitoris BA: Quantifying endocytosis in vivo using intravital two-photon microscopy. *Methods Mol Biol* 440: 389–402, 2008
13. Russo LM, Sandoval RM, Campos SB, Molitoris BA, Comper WD, Brown D: Impaired tubular uptake explains albuminuria in early diabetic nephropathy. *J Am Soc Nephrol* 20: 489–494, 2009
14. Peti-Peterdi J, Sipos A: A high-powered view of the filtration barrier. *J Am Soc Nephrol* 21: 1835–1841, 2010
15. Moeller MJ, Sanden SK, Soofi A, Wiggins RC, Holzman LB: Two gene fragments that direct podocyte-specific expression in transgenic mice. *J Am Soc Nephrol* 13: 1561–1567, 2002
16. Chaudhury C, Mehnaz S, Robinson JM, Hayton WL, Pearl DK, Roopenian DC, Anderson CL: The major histocompatibility complex-related Fc receptor for IgG (FcRn) binds albumin and prolongs its lifespan. *J Exp Med* 197: 315–322, 2003
17. Andersen JT, Dee Qian J, Sandlie I: The conserved histidine 166 residue of the human neonatal Fc receptor heavy chain is critical for the pH-dependent binding to albumin. *Eur J Immunol* 36: 3044–3051, 2006
18. Tesar DB, Björkman PJ: An intracellular traffic jam: Fc receptor-mediated transport of immunoglobulin G. *Curr Opin Struct Biol* 20: 226–233, 2010
19. Newton EE, Wu Z, Simister NE: Characterization of basolateral-targeting signals in the neonatal Fc receptor. *J Cell Sci* 118: 2461–2469, 2005
20. Haymann JP, Levraud JP, Bouet S, Kappes V, Hagège J, Nguyen G, Xu Y, Rondeau E, Sraer JD: Characterization and localization of the neonatal Fc receptor in adult human kidney. *J Am Soc Nephrol* 11: 632–639, 2000
21. Lee D, Gleich K, Fraser SA, Katerelos M, Mount PF, Power DA: Limited capacity of proximal tubular proteolysis in mice with proteinuria. *Am J Physiol Renal Physiol* 304: F1009–F1019, 2013
22. Wang B-G, König K, Halbhuber K-J: Two-photon microscopy of deep intravital tissues and its merits in clinical research. *J Microsc* 238: 1–20, 2010
23. Bliss DJ, Brewer DB: Increased albumin and normal dextran clearances in protein-overload proteinuria in the rat. *Clin Sci (Lond)* 69: 321–326, 1985
24. Lawrence GM, Brewer DB: Effect of strain and sex on the induction of hyperalbuminaemic proteinuria in the rat. *Clin Sci (Lond)* 61: 751–756, 1981
25. Davies DJ, Messina A, Thumwood CM, Ryan GB: Glomerular podocytic injury in protein overload proteinuria. *Pathology* 17: 412–419, 1985
26. Nagai J, Yamamoto A, Yumoto R, Takano M: Albumin overload induces expression of hypoxia-inducible factor 1α and its target genes in HK-2 human renal proximal tubular cell line. *Biochem Biophys Res Commun* 434: 670–675, 2013
27. Fang L, Xie D, Wu X, Cao H, Su W, Yang J: Involvement of endoplasmic reticulum stress in albuminuria induced inflammasome activation in renal proximal tubular cells. *PLoS ONE* 8: e72344, 2013
28. Gorostizaga A, Mori Sequeiros García MM, Acquier A, Gomez NV, Maloberti PM, Mendez CF, Paz C: Modulation of albumin-induced endoplasmic reticulum stress in renal proximal tubule cells by upregulation of mapk phosphatase-1. *Chem Biol Interact* 206: 47–54, 2013
29. Koltun M, Comper WD: Retention of albumin in the circulation is governed by saturable renal cell-mediated processes. *Microcirculation* 11: 351–360, 2004
30. Leheste JR, Rolinski B, Vorum H, Hilpert J, Nykjaer A, Jacobsen C, Aucouturier P, Moskaug JO, Otto A, Christensen EI, Willnow TE: Megalin knockout mice as an animal model of low molecular weight proteinuria. *Am J Pathol* 155: 1361–1370, 1999
31. Nagai J, Christensen EI, Morris SM, Willnow TE, Cooper JA, Nielsen R: Mutually dependent localization of megalin and Dab2 in the renal proximal tubule. *Am J Physiol Renal Physiol* 289: F569–F576, 2005
32. Tojo A, Kinugasa S: Mechanisms of glomerular albumin filtration and tubular reabsorption. *Int J Nephrol* 481520: 2012
33. Guasch A, Deen WM, Myers BD: Charge selectivity of the glomerular filtration barrier in healthy and nephrotic humans. *J Clin Invest* 92: 2274–2282, 1993
34. Storm T, Tranebjærg L, Frykholm C, Birn H, Verroust PJ, Névéus T, Sundelin B, Hertz JM, Holmström G, Ericson K, Christensen EI, Nielsen R: Renal phenotypic investigations of megalin-deficient patients: novel insights into tubular proteinuria and albumin filtration. *Nephrol Dial Transplant* 28: 585–591, 2013

35. Böger CA, Chen M-H, Tin A, Olden M, Köttgen A, de Boer IH, Fuchsberger C, O'Seaghdha CM, Pattaro C, Teumer A, Liu CT, Glazer NL, Li M, O'Connell JR, Tanaka T, Peralta CA, Kutalik Z, Luan J, Zhao JH, Hwang SJ, Akylbekova E, Kramer H, van der Harst P, Smith AV, Lohman K, de Andrade M, Hayward C, Kollerits B, Tönjes A, Aspelund T, Ingelsson E, Eiriksdottir G, Launer LJ, Harris TB, Shuldiner AR, Mitchell BD, Arking DE, Franceschini N, Boerwinkle E, Egan J, Hernandez D, Reilly M, Townsend RR, Lumley T, Siscovick DS, Psaty BM, Kestenbaum B, Haritunians T, Bergmann S, Vollenweider P, Waeber G, Mooser V, Waterworth D, Johnson AD, Florez JC, Meigs JB, Lu X, Turner ST, Atkinson EJ, Leak TS, Aasarød K, Skorpen F, Syvänen AC, Illig T, Baumert J, Koenig W, Krämer BK, Devuyst O, Mychaleckyj JC, Minelli C, Bakker SJ, Kedenko L, Paulweber B, Coassin S, Endlich K, Kroemer HK, Biffar R, Stracke S, Völzke H, Stumvoll M, Mägi R, Campbell H, Vitart V, Hastie ND, Gudnason V, Kardia SL, Liu Y, Polasek O, Curhan G, Kronenberg F, Prokopenko I, Rudan I, Arnlöv J, Hallan S, Navis G, Parsa A, Ferrucci L, Coresh J, Shlipak MG, Bull SB, Paterson NJ, Wichmann HE, Wareham NJ, Loos RJ, Rotter JI, Pramstaller PP, Cupples LA, Beckmann JS, Yang Q, Heid IM, Rettig R, Dreisbach AW, Bochud M, Fox CS, Kao WH; CKDGen Consortium: CUBN is a gene locus for albuminuria. *J Am Soc Nephrol* 22: 555–570, 2011

36. Ovunc B, Otto EA, Vega-Warner V, Saisawat P, Ashraf S, Ramaswami G, Fathy HM, Schoeb D, Chernin G, Lyons RH, Yilmaz E, Hildebrandt F: Exome sequencing reveals cubilin mutation as a single-gene cause of proteinuria. *J Am Soc Nephrol* 22: 1815–1820, 2011

37. Amsellem S, Gburek J, Hamard G, Nielsen R, Willnow TE, Devuyst O, Nexo E, Verroust PJ, Christensen EI, Kozyraki R: Cubilin is essential for albumin reabsorption in the renal proximal tubule. *J Am Soc Nephrol* 21: 1859–1867, 2010

38. Kuo TT, de Muinck EJ, Claypool SM, Yoshida M, Nagaishi T, Aveson VG, Lencer WI, Blumberg RS: N-glycan moieties in neonatal Fc receptor determine steady-state membrane distribution and directional transport of IgG. *J Biol Chem* 284: 8292–8300, 2009

39. McCarthy KM, Lam M, Subramanian L, Shakya R, Wu Z, Newton EE, Simister NE: Effects of mutations in potential phosphorylation sites on transcytosis of FcRn. *J Cell Sci* 114: 1591–1598, 2001

40. Dickinson BL, Claypool SM, D'Angelo JA, Aiken ML, Venu N, Yen EH, Wagner JS, Borawski JA, Pierce AT, Hershberg R, Blumberg RS, Lencer WI: Ca2+-dependent calmodulin binding to FcRn affects immunoglobulin G transport in the transcytotic pathway. *Mol Biol Cell* 19: 414–423, 2008

41. Marzolo M-P, Yuseff MI, Retamal C, Donoso M, Ezquer F, Farfán P, Li Y, Bu G: Differential distribution of low-density lipoprotein-receptor-related protein (LRP) and megalin in polarized epithelial cells is determined by their cytoplasmic domains. *Traffic* 4: 273–288, 2003

42. Zhang H, Yoshioka S, Miyazaki M, Kannagi R, Suzuki A: Core 2 GlcNAc modification and megalin ligand-binding activity. *Biochim Biophys Acta* 1780: 479–485, 2008

43. Yuseff MI, Farfan P, Bu G, Marzolo M-P: A cytoplasmic PPPSP motif determines megalin's phosphorylation and regulates receptor's recycling and surface expression. *Traffic* 8: 1215–1230, 2007

44. Coudroy G, Gburek J, Kozyraki R, Madsen M, Trugnan G, Moestrup SK, Verroust PJ, Maurice M: Contribution of cubilin and amnionless to processing and membrane targeting of cubilin-amnionless complex. *J Am Soc Nephrol* 16: 2330–2337, 2005

45. Aseem O, Barth JL, Klatt SC, Smith BT, Argraves WS: Cubilin expression is monoallelic and epigenetically augmented via PPARs. *BMC Genomics* 14: 405, 2013

46. Sarav M, Wang Y, Hack BK, Chang A, Jensen M, Bao L, Quigg RJ: Renal FcRn reclaims albumin but facilitates elimination of IgG. *J Am Soc Nephrol* 20: 1941–1952, 2009

47. Hosaka K, Takeda T, Iino N, Hosojima M, Sato H, Kaseda R, Yamamoto K, Kobayashi A, Gejyo F, Saito A: Megalin and nonmuscle myosin heavy chain IIA interact with the adaptor protein Disabled-2 in proximal tubule cells. *Kidney Int* 75: 1308–1315, 2009

48. Koral K, Erkan E: PKB/Akt partners with Dab2 in albumin endocytosis. *Am J Physiol Renal Physiol* 302: F1013–F1024, 2012

49. Williams DB: Beyond lectins: the calnexin/calreticulin chaperone system of the endoplasmic reticulum. *J Cell Sci* 119: 615–623, 2006

50. Wu VY, Shearman CW, Cohen MP: Identification of calnexin as a binding protein for Amadori-modified glycated albumin. *Biochem Biophys Res Commun* 284: 602–606, 2001

51. Hall AM, Campanella M, Loesch A, Duchen MR, Unwin RJ: Albumin uptake in OK cells exposed to rotenone: a model for studying the effects of mitochondrial dysfunction on endocytosis in the proximal tubule? *Nephron Physiol* 115: p9–p19, 2010

52. Shelton LM, Park BK, Copple IM: Role of Nrf2 in protection against acute kidney injury. *Kidney Int* 84: 1090–1095, 2013

53. Kurniati NF, van Meurs M, Vom Hagen F, Jongman RM, Moser J, Zwiers PJ, Struys MMRF, Westra J, Zijlstra JG, Hammes H-P, Molema G, Heeringa P: Pleiotropic effects of angiopoietin-2 deficiency do not protect mice against endotoxin-induced acute kidney injury. *Nephrol Dial Transplant* 28: 567–575, 2013

54. Yuan HT, Khankin EV, Karumanchi SA, Parikh SM: Angiopoietin 2 is a partial agonist/antagonist of Tie2 signaling in the endothelium. *Mol Cell Biol* 29: 2011–2022, 2009

55. Molnar MZ, Kümpers P, Kielstein JT, Schiffer M, Czira ME, Ujszaszi A, Kovesdy CP, Mucsi I: Circulating Angiopoietin-2 levels predict mortality in kidney transplant recipients: a 4-year prospective case-cohort study. *Transpl Int* 27: 541–552, 2014

56. Zahr NM, Bell RL, Ringham HN, Sullivan EV, Witzmann FA, Pfefferbaum A: Ethanol-induced changes in the expression of proteins related to neurotransmission and metabolism in different regions of the rat brain. *Pharmacol Biochem Behav* 99: 428–436, 2011

57. Candiano G, Bruschi M, Musante L, Santucci L, Ghiggeri GM, Carnemolla B, Orecchia P, Zardi L, Righetti PG: Blue silver: a very sensitive colloidal Coomassie G-250 staining for proteome analysis. *Electrophoresis* 25: 1327–1333, 2004

58. Koehler G, Wilson RC, Goodpaster JV, Sønsteby A, Lai X, Witzmann FA, You J-S, Rohloff J, Randall SK, Alsheikh M: Proteomic study of low-temperature responses in strawberry cultivars (Fragaria x ananassa) that differ in cold tolerance. *Plant Physiol* 159: 1787–1805, 2012

59. Keller A, Nesvizhskii AI, Kolker E, Aebersold R: Empirical statistical model to estimate the accuracy of peptide identifications made by MS/MS and database search. *Anal Chem* 74: 5383–5392, 2002

60. Nesvizhskii AI, Keller A, Kolker E, Aebersold R: A statistical model for identifying proteins by tandem mass spectrometry. *Anal Chem* 75: 4646–4658, 2003

61. Najjar F, Zhou H, Morimoto T, Bruns JB, Li H-S, Liu W, Kleyman TR, Satlin LM: Dietary K+ regulates apical membrane expression of maxi-K channels in rabbit cortical collecting duct. *Am J Physiol Renal Physiol* 289: F922–F932, 2005